Role of IgM and IgA Antibodies to the Neutralization of SARS-CoV-2

Jéromine Klingler[1,2], Svenja Weiss[1,2], Vincenza Itri[1], Xiaomei Liu[1,2], Kasopefoluwa Y. Oguntuyo[3], Christian Stevens[3], Satoshi Ikegame[3], Chuan-Tien Hung[3], Gospel Enyindah-Asonye[1], Fatima Amanat[3,4], Ian Baine[5], Suzanne Arinsburg[5], Juan C. Bandres[2], Erna Milunka Kojic[6], Jonathan Stoever[7], Denise Jurczyszak[3,4], Maria Bermudez-Gonzalez[3], Viviana Simon[1,3,8], Sean Liu[1,3], Benhur Lee[3], Florian Krammer[3], Susan Zolla-Pazner[1,3*], Catarina E. Hioe[1,2,3*]

[1]Division of Infectious Diseases, Department of Medicine, Icahn School of Medicine at Mount Sinai, New York, NY U.S.A.

[2]James J. Peters VA Medical Center, Bronx, NY, U.S.A.

[3]Department of Microbiology, Icahn School of Medicine at Mount Sinai, New York, NY, U.S.A.

[4]Graduate School of Biomedical Sciences, Icahn School of Medicine at Mount Sinai, New York, NY, U.S.A.

[5]Department of Pathology, Icahn School of Medicine at Mount Sinai, New York, NY, U.S.A.

[6]Division of Infectious Diseases, Department of Medicine, Mount Sinai West and Morningside, NY, U.S.A.

[7]Pulmonary and Critical Care Medicine, Mount Sinai West, NY, U.S.A.

[8]Global Health Emerging Pathogens Institute, Icahn School of Medicine at Mount Sinai, NY, U.S.A.

*Co-corresponding author

Contact: catarina.hioe@mssm.edu, catarina.hioe@va.gov

Abstract

SARS-CoV-2 has infected millions of people and is on a trajectory to kill more than one million globally. Virus entry depends on the receptor-binding domain (RBD) of the spike protein. Although previous studies demonstrated anti-spike and -RBD antibodies as essential for protection and convalescent plasma as a promising therapeutic option, little is known about the immunoglobulin (Ig) isotypes capable of blocking virus entry. Here, we studied spike- and RBD-specific Ig isotypes in plasma/sera from two acutely infected and 29 convalescent individuals. Spike- and RBD-specific IgM, IgG1, and IgA1 antibodies were produced by all or nearly all subjects at varying levels and detected at 7-8 days post-disease onset. IgG2, IgG3, IgG4, and IgA2 were also present but at much lower levels. All samples also displayed neutralizing activity. IgM, IgG, and IgA were capable of mediating neutralization, but neutralization titers correlated better with binding levels of IgM and IgA1 than IgG.

Background

In December 2019, the first patients with coronavirus disease 2019 (COVID-19), caused by severe acute respiratory syndrome coronavirus 2 (SARS-CoV-2) were identified in the city of Wuhan, Hubei Province, China[1]. Since then, the epidemic has rapidly spread to most regions of the world, infecting millions of people[2]. Effective therapeutics and vaccines against SARS-CoV-2 are urgently needed. To this end, more information about the Ig isotypes present in the plasma of COVID-19 convalescent individuals and their antiviral activities are needed, as convalescent plasma transfusion showed promising results in patients with severe to life-threatening COVID-19[3–5]. The data would also inform vaccine development, as more than 100 vaccine candidates are in different stages of preclinical development, and many are now in phase 2 and 3 clinical trials[6]. Although using different strategies[7], many vaccines are based on one of the three membrane-anchored proteins present on the virus envelope surface: the SARS-CoV-2 spike protein[8,9], which contains the receptor-binding domain (RBD) required for binding to and entry into the cells[10–17]. These vaccines aim to protect by inducing neutralizing antibodies (Abs) capable of blocking the viral infection. However, which of the immunoglobulin (Ig) isotypes are protective is not yet clear.

Monomeric IgG constitutes approximately 75% of the Abs found in serum and exists as four subtypes: IgG1 (~66% of IgG), IgG2 (~23% of IgG), IgG3 (~7% of IgG) and IgG4 (~4% of IgG)[18,19]. IgM Abs represent 10% of total serum Abs and are the first to arise in response to new antigens[19,20]. Although IgM Abs do not undergone extensive somatic hypermutation to increase their affinity as do IgG and IgA Abs, their higher valency due to the oligomerization of IgM enhances their avidity and potency against pathogens[19,21,22]. IgA Abs exist as two subtypes: IgA1 and IgA2, and represent 15% of total serum Abs[19]. They are dimeric in the mucosa, but in the circulation, these two IgA subtypes are monomeric.

SARS-CoV-2 spike-, RBD- and nucleocapsid-specific serum/plasma Abs of IgM, IgG, and IgA

isotypes are found in most COVID-19 patients[23–30], with Ab neutralizing activities reported among the convalescent patients[26,28,31,32]. However, the neutralizing titers appear to vary greatly[26,28,31,32] and they correlate with Ab binding levels against RBD, spike, and/or nucleocapsid, and also with age, duration of symptoms, and symptom severity[26,28,32]. Several RBD-specific monoclonal Abs of IgG isotype with potent antiviral activities has been generated from individuals with high neutralization titers and these confer protection in animal models[26,31,33,34]. Moreover, a monoclonal Ab of IgA isotype capable of recognizing both the SARS-CoV-1 and SARS-CoV-2 spike proteins, and blocking ACE2 receptor binding was recently described[35]. However, no data are available regarding the neutralizing capacity of plasma IgM and IgA Abs from COVID-19 patients.

Studies on other respiratory viruses such as influenza show that, in addition to IgG, IgA could also mediate virus neutralization, and their relative contribution depends on the physiologic compartment in which they are found, with IgA contributing to the protection of mostly the upper respiratory tract while IgG was protecting the lower respiratory tract[36–39]. Of note, an anti-hemagglutinin monoclonal IgA has been demonstrated to mediate more potent antiviral activities against influenza when compared to a monoclonal IgG against the same epitope[40]. Interestingly, an IgM Ab with potent antiviral activities targeting the receptor binding site of influenza B has also been described[41]. In addition, mucosal respiratory syncytial virus (RSV)-specific IgA neutralizing Abs is a better correlate of protection than serum RSV-specific IgG neutralizing Abs[42]. In the case of SARS-CoV-1, high titers of mucosal IgA in the lungs are correlated with reduced pathology upon viral challenge in animal models[43]. Whether IgA in the blood and the respiratory tract mucosa offers protection against SARS-CoV-2 infection remains an open question. Moreover, few data are available concerning the contribution of IgM to neutralization and protection against viruses, including SARS-CoV-2.

We have recently published a Luminex assay detecting Ig total against spike and RBD[44]. Based on this assay, we studied here the Ig isotype profiles against spike and RBD in the plasma and serum

from acutely infected or convalescent individuals using a Luminex assay that detects antigen-specific IgM, IgG1-4, IgA1 and IgA2. Using a pseudovirus assay[45], we also measured neutralizing activities in plasma and serum samples and in Ig isotype fractions to determine the neutralizing capacity of IgM, IgA, and IgG. The data demonstrate high prevalence of spike- and RBD-specific IgM and IgA, similar to that of IgG1, in plasma/serum from COVID-19 patients and their significant contributions to virus-neutralizing activities. This is the first evidence that purified plasma IgG, IgM, and IgA contributes to SARS-CoV-2 neutralization.

Results

Levels of Ig isotypes against the SARS-CoV-2 spike and RBD vary in convalescent individuals. A total of 29 serum (P#5-8) and plasma (TF#1-25) specimens from COVID-19-convalescent individuals was tested. Sera from three uninfected individuals banked as part of an ongoing longitudinal study prior to the COVID-19 outbreak (N#1-3), and an additional ten plasma from COVID-negative contemporaneous blood bank donors (N#4-13) were included for comparison. The specimens were initially titrated for total Ig against spike and RBD (**Fig. 1**). All 29 COVID-19 positive specimens exhibited titration curves of total Ig Abs against spike, while none of the negative controls did. Similar results were observed with RBD, except that one COVID-19-negative sample had low titrating levels of RBD-specific Ig. Overall the background MFI values were higher for RBD than spike. The areas under curves (AUCs) highly correlated with the 1:200 dilution MFI ($p < 0.0001$; **Supplementary Fig. 1**), consequently all samples were tested for isotyping at this dilution. To assess the reproducibility of the assay, the samples were tested in at least two separate experiments run on different days, and a strong correlation was observed between the MFIs from these independent experiments (**Supplementary Fig. 2**). To evaluate for the presence of spike-specific and RBD-specific total Ig, IgM, IgG1, IgG2, IgG3, IgG4, IgA1 and IgA2, the specificity of the secondary Abs used to detect the different isotypes were first validated with Luminex beads coated with myeloma proteins of known Ig isotypes (IgG1, IgG2, IgG3,

IgG4, IgA1, IgA2, and IgM) (**Supplementary Fig. 3**).

While all 29 convalescent individuals had anti-spike and anti-RBD total Ig (**Fig. 2**), the Ig levels were highly variable, with MFI values ranging from 36,083 to 190,150. All 29 convalescent individuals displayed IgM Abs against spike at varying levels, although only 55% (16/29) were positive for anti-RBD IgM, when evaluated using cut-off values calculated as mean + 3 standard deviation (SD) of the 13 COVID-negative samples. The lower percentage of IgM Abs specific for RBD might be due to the high background observed for IgM against RBD with COVID-negative specimens (**Fig. 2b,c**). An IgG1 response was also detected against both spike and RBD in 97% of the convalescent subjects, with MFI values that ranged from 1012.5 to 59,880, and the responses against spike and RBD were highly correlated for every isotype (**Supplementary Fig. 4**). In contrast IgG2, IgG3, and IgG4 Abs against spike and RBD were detected in only a small fraction of the subjects, and the levels were very low (MFI values < 1300) (**Fig. 2**).

Surprisingly, almost all the individuals produced IgA1 Abs against spike (90%) and RBD (86%) while 21% exhibited IgA2 against spike, and 48% exhibited IgA2 against RBD (**Fig. 2**). Overall, these data demonstrate that IgM, IgG1, and IgA1 Abs were all strongly induced against spike and RBD in all or almost all COVID-19 convalescent individuals (**Fig. 2**). The levels, however, were highly variable among individuals. While not reaching statistical significance, a general trend was observed toward higher levels of total Ig, IgM, IgG1, and IgA1 in women compared to men (**Supplementary Fig. 5**). In **Fig. 3**, comparing levels of total Ig with the different Ig isotypes showed a highly significant correlation with IgG1 for both Abs specific for spike and RBD indicating that IgG1 is the major isotype induced by SARS-CoV-2 infection. There was no other isotype which showed a significant correlation with total Ig Abs for anti-spike Abs, although there was a significant correlation between total Ig and IgA1 for anti-RBD Abs. Moreover, none of the IgM, IgG1, or IgA1 isotypes correlated with one another (**Fig. 3c**).

IgA1 is induced early after disease onset in COVID-19 patients. Since almost all convalescent

COVID-19 patients displayed IgA Ab responses to spike and RBD antigens, we sought to evaluate the kinetics of IgA versus other Ig isotype induction at early time points. We tested longitudinal samples collected from two patients (P#1 and P#2) from days 7 to 15 post-onset of symptoms. The earliest samples from both patients were positive for IgA1 Abs against spike (**Fig. 4a**) and RBD (**Fig. 4b**), and the levels increased over time. Like IgA1 Ab, total Ig, IgM, and IgG1 Abs were also detectable as early as 7-8 days post symptom onset, and their levels increased over time. On the contrary, IgA2 Ab levels were near or below background on days 7-8 and remained unchanged over two weeks post-onset. IgG4 Abs also remained low or near background, whereas IgG2 and IgG3 Abs increased slightly to above background after 10-15 days.

Neutralizing activities is detected in all convalescent COVID-19 individuals. We subsequently tested the ability of samples from convalescent subjects to neutralize a VSVΔG pseudovirus bearing the SARS-CoV-2 spike protein (COV2pp). The results, shown in **Fig. 5** demonstrate the percentage of COV2pp neutralizing activity in serum or plasma specimens from 28 COVID-19-convalescent individuals and 11 COVID-19-negative individuals over a range of seven serial 4-fold dilutions. Soluble recombinant RBD (sRBD) was tested in parallel as a positive control.

All specimens from COVID-19-convalescent individuals were able to neutralize the virus at levels superior to 50% (**Fig. 5a**). For 26 of 28 specimens, neutralization reached more than 90% (**Fig. 5a**). Interestingly, one sample demonstrated highly potent neutralization with a reciprocal IC_{50} titer > 40,960, and neutralization was still 75% at the highest dilution tested. In contrast, one sample had a low neutralization titer (reciprocal IC_{50} titer = 37) and reached a neutralization plateau of only ~60%. In comparison, none of the samples from COVID-19-negative individuals reached 50% neutralization (**Fig. 5b**), while the sRBD positive control demonstrated potent neutralization with an IC_{50} of 0.06 μg/mL (**Fig. 5c**), similar to that recently reported[45].

SARS-CoV-2 neutralization titers correlate with IgM and IgA1. Given our observation that Ab

isotype levels and neutralization titers varied tremendously among convalescent COVID-19 individuals (**Fig. 6**), we investigated if neutralizing activities correlated with a particular Ab isotype. IgM Abs specific for spike and RBD displayed the strongest correlation with neutralizing Abs ($p < 0.0001$ and $p = 0.0002$, respectively), while IgG1 did not show a significant correlation (**Fig. 7a)**. Neutralization reciprocal IC_{90} titers weakly correlated with RBD-specific total Ig levels but did not correlate with spike-specific total Ig levels (**Fig. 7a**). Correlation with IC_{50} titers yielded similar results (data not shown). IgA1 levels also correlated with reciprocal IC_{90} titers ($p = 0.013$ and $p = 0.006$ for spike and RBD, respectively; **Fig. 7a**). Although there were significant correlations between anti-spike and -RBD Abs of the IgG2 and IgG3s isotypes, most of the neutralization values were below the cut-off and for the few IgG3 and IgG2 responders, the levels were near background (**Fig. 7b**).

Neutralizing activities are mediated by IgM, IgG, and IgA fractions. The data above show the strongest correlation of neutralizing activity with IgM. To ask directly to what extent Abs of different isotypes mediate neutralization, we evaluated the neutralization activities of IgM, IgG, and IgA fractions purified from plasma from five COVID-19-convalescent individuals (RP#1-5). The enrichment of IgM, IgG1, and IgA1 Abs reactive with spike and RBD was validated using the isotyping method used above (**Supplementary Fig. 6** and not shown). These IgM, IgG and IgA fractions were then evaluated for neutralizing activity along with the original plasma (**Fig. 8**). The RP#1-5 plasma neutralizing reciprocal IC50 titers ranged from 35 to 690 (**Fig. 8a,b**). The purified IgG, IgA and IgM fractions all displayed neutralization of more than 50%, while the negative control Ig fractions (RN#1) did not (**Fig. 8c,d**). The IC_{50} values for IgM and IgG were similar, and both were significantly better than IgA (**Fig 8c,d**).

Discussion

Our study demonstrates the presence of IgG1, IgA1 and IgM within 7-8 days after the onset of symptom, and the correlation of neutralizing activity is strongest with IgM, followed by IgA1, but does not correlate with IgG1 or other IgG isotypes. While correlations are important, direct testing of

neutralizing activities of different isotypes was performed, and these experiments showed that neutralizing activity was displayed most potently by IgM and IgG and less strongly by IgA. These data indicate the protective potential of all three major Ig isotypes and suggest that induction of each of these isotypes by vaccination may offer optimal protection against infection. These data also carry important implications for the use of hyperimmune globulin as treatment and prophylactic modalities.

Several SARS-CoV-2 vaccine candidates tested in animal models and humans were shown to induce IgG responses against spike and RBD as well as virus neutralizing activities, but in many of these studies, the induction of other Ig isotypes was not evaluated[46–49]. DNA vaccines expressing full-length and truncated spike proteins were able to curtail virus infection in the respiratory tract by varying degrees. Virus reduction correlated with levels of neutralization and also Fc-mediated effector functions such as antibody-dependent complement deposition (ADCD)[9]. Interestingly, these DNA vaccines elicited spike- and RBD-specific IgG1, IgG2, IgG3, IgA, and IgM Abs, and similar to our findings, neutralization correlated most strongly with IgM. Adenovirus serotype 26 vaccine vectors encoding seven different SARS-CoV-2 spike variants showed high protection, and virus reduction correlated best with neutralizing Ab titers together with IgM binding levels, FcγRII-binding, and ADCD responses[50]. We noted that while all COVID-19 convalescent individuals exhibited plasma/serum neutralization activities, reaching 50% neutralization, and 26 of 28 specimens attained 90% neutralization, neutralization levels were highly variable with reciprocal IC_{50} and IC_{90} titers ranging over three orders of magnitude. Similarly, the levels of spike- and RBD-binding total Ig and Ig isotypes also varied greatly. A trend to higher levels of total Ig and each Ig isotype was seen in female compared to male subjects, as reported in another study[51]. Moreover, except for TF#11 (a male elite neutralizer), the median neutralizing reciprocal IC_{90} titer was higher in females than males, although the difference did not reach significance (data not shown). Gender differences in Ab induction have been observed following vaccination against influenza in humans and mice and were shown to result from the impact

of sex steroids[52,53]. Whether and to what extent this contributes to gender differences seen in clinical outcomes of COVID-19[54] remains to be investigated. Other studies have shown that the Ab levels were associated with multiple factors, including time from disease onset[55] and disease severity[25]. However, clinical data are not available for the subjects studied here, limiting our analysis only to neutralization and Ig isotypes.

One remarkable finding from our study is that neutralization levels correlated with binding levels of IgM and IgA1, but not IgG1. This is consistent with our data showing the neutralization activities mediated by purified IgM and IgA fractions from COVID-19 patients. Nonetheless, purified IgG fractions from convalescent plasma also exhibited potent neutralization, but since the fractions contained all four IgG subtypes, it remains unknown which IgG subtypes contribute to neutralization, although IgG1, the most abundant IgG isotypes in the blood, did not correlate with neutralization titers, and IgG2 and IgG3 present at low levels displayed weak correlations. The lack of correlation between IgG1 binding titers and neutralization activities may be explained by the fact that the dominant IgG1 responses may target sites not critical for blocking virus entry. Indeed, among mAbs isolated from six COVID-19 convalescent patients, > 40% of RBD-specific mAbs did not display neutralizing activities[26] and another study demonstrated that mAbs that bind to non-RBD epitopes on the spike protein had poor neutralization potencies[33]. Nonetheless, the absence of a correlation between IgG1 binding titers and neutralizing activities reported above requires more study given that data remain controversial since other studies have demonstrated correlations between neutralization titers and SARS-CoV-2 specific IgG levels[26,28,32].

In addition to neutralization, non-neutralizing Ab activities have been implicated in protection from virus infection through potent Fc-mediated functions such as antibody-dependent cellular cytotoxicity (ADCC), antibody-dependent cellular phagocytosis (ADCP), and complement-mediated lysis; this is true for HIV, influenza, Marburg, and Ebola viruses[38,56–59]. These Fc activities were not evaluated in our

study, and their contribution to protection against infection and disease progression in humans is yet unclear[9,60,61]. Interestingly, a recent study demonstrated enrichment of spike-specific IgM and IgA1 Abs and spike-specific phagocytic and ADCD activity in plasma of individuals who recovered from infection, while nucleocapsid-specific IgM and IgA2 responses and nucleocapsid-specific ADCD activity were features enriched in deceased patients[62]. Defining the full potential of Abs against SARS-CoV-2 that includes neutralizing, non-neutralizing and enhancing activities is vital for developing the most effective vaccines and determining the optimal convalescent Ab treatment against COVID-19.

When we examined plasma specimens collected within 7-8 days after COVID-19 onset, we detected IgG and IgA against spike and RBD, as well as IgM. This is consistent with published reports showing that 100% of COVID-19-infected individuals developed IgG within 19 days after symptom onset and that seroconversion for IgG and IgM occurred simultaneously or sequentially[25]. IgA was also found early after infection (4-6 days after symptom onset) in another study[23]. These studies suggest that measuring total Ig, rather than IgG, would provide a better outcome for diagnosis of early disease. Indeed, we found no correlation between the levels of different isotypes examined in our study. This lack of correlation may result from their non-synchronous, sequential induction (IgM first, then IgG, and finally IgA), but the presence of IgA early during acute infection also suggests the potential contribution of natural IgA, which, similar to natural IgM, arise spontaneously from innate B1 cells to provide the initial humoral responses before the induction, maturation, and class-switching of adaptive classical B cells[63,64].

In summary, this study demonstrates that spike- and RBD-specific IgM, IgG1, and IgA1 Abs were present in serum or plasma of all or almost all analyzed COVID-19 convalescent subjects and were detected at extremely early stages of infection. The plasma of convalescent individuals also displayed neutralization activities that were mediated by IgM, IgG, and IgA1, although neutralization titers correlated more strongly with levels of IgM and IgA1 than IgG. The contribution of IgM and IgA Abs to

the neutralizing activities against SARS-CoV-2 demonstrates their importance of protective immunity against this virus.

Methods

Recombinant proteins. The recombinant spike and RBD proteins were produced as previously described[65] in Expi293F cells (ThermoFisher) by transfections of purified D.N.A. using an ExpiFectamine Transfection Kit (ThermoFisher). The soluble version of the spike protein included the protein ectodomain (amino acids 1-1213), a C-terminal thrombin cleavage site, a T4 foldon trimerization domain, and a hexahistidine tag. The protein sequence was also modified to remove the polybasic cleavage site (RRAR to A) and two stabilizing mutations (K986P and V987P, wild type numbering). The RBD (amino acids 319-541) included the signal peptide (amino acids 1–14) and a hexahistidine tag. Supernatants from transfected cells were harvested on day three post-transfection by centrifugation of the culture at 4000 g for 20 min. The supernatant was then incubated with 6 mL Ni-NTA agarose (Qiagen) for one to two hours at room temperature. Next, gravity-flow columns were used to collect the Ni-NTA agarose, and the protein was eluted. Each protein was concentrated in Amicon centrifugal units (E.M.D. Millipore) and resuspended in phosphate buffered saline (PBS).

Human samples. Twenty-five citrated plasma of convalescent COVID-19 individuals destined for transfusion to SARS-CoV-2-infected individuals (TF#1-25) were obtained from the Division of Transfusion Medicine of the Department of Pathology, Molecular and Cell-Based Medicine. A pool of 0.1 mL from ten of these specimens was used as a positive control in each experiment. An additional ten specimens were derived from the blood bank (N#4-13), representing current COVID-19-negative blood bank donors. A pool of 0.1 mL from ten of these specimens was used as a negative control in each experiment. Four additional de-identified serum specimens from individuals with COVID-19 (P#5-8) were provided by the Clinical Pathology Division of the Department of Pathology, Molecular and Cell-Based Medicine at the Icahn School of Medicine at Mount Sinai. Serum and plasma samples were also

obtained from study participants enrolled in IRB-approved protocols at Icahn School of Medicine at Mount Sinai and the James J. Peter VA Medical Center. Study participants provided written consent at enrollment and agreed to sample banking and future research use of their banked biospecimen. Samples from these protocols included sera from seven participants with documented SARS-CoV-2 infection: specimens from P#1 (d8, d11, and d15 after symptom onset), P#2 (d7, and d10 after symptom onset), and RP#1-5. In addition, sera were used, which had been collected from healthy donors prior to the spread of SARS-CoV-2 in the U.S.A.

Ig fractionation. IgA was first isolated from plasma by mixing 1:2 diluted plasma with peptide M agarose beads (600 µL/28 mL plasma, InvivoGen #GEL-PDM) for 1.5 hours at room temperature. Beads were then collected on a column and washed with PBS until protein reading (280 nm) by Nanodrop reached background. IgA was eluted from beads with a pH 2.8 elution buffer (Thermo Scientific #21004) and neutralized with pH 9 Tris buffer. The pass-through plasma sample was collected for IgG enrichment using protein G agarose beads (InvivoGen #GEL-AGG) using the same protocol as above and subsequently for IgM isolation using a HiTrap IgM column (G.E. Healthcare #17-5110-01) according to the manufacturer's instruction. An additional purification step was performed using Protein A Plus mini-spin columns to separate IgG from IgM. Protein concentrations were determined with Nanodrop prior to use in Luminex and neutralization experiments.

Luminex binding Ab assay. The SARS-CoV-2 antigens used in this assay were a soluble recombinant trimerized form of the spike protein and a recombinant RBD protein[66]. Antigens were coupled as previously described, with minor changes[44]. Each antigen was covalently coupled individually to a uniquely labeled fluorochrome carboxylated xMAP bead set at 2.0 µg protein/million beads using a two-step carbodiimide reaction with the xMAP Ab Coupling (AbC) Kit following to the manufacturers' instructions (Luminex, Austin, TX). The coupled beads were pelleted, resuspended at $5x10^6$ beads/mL in storage buffer (PBS, 0.1% bovine serum albumin (B.S.A.), 0.02% Tween-20, and 0.05% sodium azide,

pH 7.4), and stored at -80°C. Three to five million beads per batch were prepared in a 1.5 mL conical tube.

Before each experiment, the beads needed for a single run (2,500 beads/well x number of wells) were pelleted and resuspended in assay buffer (PBS, 0.1% B.S.A., 0.02% Tween-20) to deliver 2,500 beads in a volume of 50 µL/well. Sera/plasma samples were serially titrated (1:50 to 1:6400 final dilution) or diluted in assay buffer to 1:100 (for a final dilution of 1:200). The samples were then added as 50 µL/well to the wells containing the beads and incubated at room temperature for 1 hour at 600 rpm. After two washes in assay buffer, 100 µL/well of biotinylated antibodies specific for total Ig, IgG1, IgG2, IgG3, IgG4, IgA1, IgA2, or IgM was added and incubated for 30 min at room temperature on a plate shaker; these antibodies were rabbit biotinylated-anti-human total Ig (Abcam, catalog #ab97158) at 2 µg/mL, mouse biotinylated-anti-human IgG1 Fc (Invitrogen #MH1515) at 4 µg/mL, mouse biotinylated-anti-human IgG2 Fc (Southern Biotech #9060-08) at 1 µg/mL, mouse biotinylated-anti-human IgG3 Hinge (Southern Biotech #9210-08) at 3 µg/mL, mouse biotinylated-anti-human IgG4 Fc (Southern Biotech #9200-08) at 4 µg/mL, mouse biotinylated-anti-human IgA1 Fc (Southern Biotech #9130-08) at 4 µg/mL, mouse biotinylated-anti-human IgA2 Fc (Southern Biotech #9140-08) at 4 µg/mL or goat biotinylated-anti-human IgM (Southern Biotech #2020-08) at 3 µg/mL. After two washes, 100 µL/well of Streptavidin-Phycoerythrin (P.E.) at 1 µg/mL was added (BioLegend #405204) followed by a 30 min incubation at room temperature on a plate shaker. After two additional washes, 100 µL of assay buffer/well was added and put on a shaker to resuspend the beads. The plate was read with a Luminex Flexmap 3D instrument. Specimens were tested in duplicate, and the results were recorded as mean fluorescent intensity (MFI).

COV2pp production and titration. The SARS-CoV-2 pseudovirus (COV2pp) was produced as previously described[45]. Briefly, 293T cells were transfected to overexpress SARS-CoV-2 glycoproteins. For background entry with particles lacking a viral surface glycoprotein, pCAGG empty vector was

transfected into 293T cells. Around 8 hours post-transfection, cells were infected with the VSVΔG-rLuc reporter virus for 2 hours, and then washed with PBS. Two days post-infection, supernatants were collected and clarified by centrifugation at 1250 rpm for 5 minutes. At the time of collection, a small batch of VSVΔG-rLuc particles bearing the CoV2pp were treated with TPCK-treated trypsin (Sigma-Aldrich #T1426-1G) at room temperature for 15 minutes prior to inhibition with soybean trypsin inhibitor (Fisher Scientific #1707502). Finally, particles were aliquoted prior to storage in -80°C.

The pseudoviruses were titrated on 20,000 Vero-CCL81 cells seeded in a 96-well black plate with clear bottom 24 hours before infection. At 18 to 22 hours post-infection, the infected cells were washed with PBS and processed for detection of Renilla luciferase activity with Renilla-Glo™ Luciferase Assay System (Promega #E2720). A Cytation3 (BioTek) instrument was used to read luminescence.

COV2pp neutralization. The day before infection, 20,000 Vero-CCL81 cells per well were seeded in a 96-well black plate with clear bottom. On the assay day, the COV2pp was diluted based on the titration results, and 82.5 µL added to all wells, except 6 for cell control, of a 96-well V-bottom plate. The seven serial dilutions of the samples were then prepared in another 96-well V-bottom plate. Samples of the COVID-19-infected individuals and COVID-19-negative individuals were tested at 4-fold dilutions from 1:10 to 1:40,960. Purified IgM, IgG, and IgA fractions and a negative control Ig fraction were tested at 4-fold dilutions from 500 to 0.02 µg/mL. 27.5 µL per well of the diluted sample was then added to the plate with the pseudovirus. For each plate, six wells were kept with the virus only, as virus control, and six wells with media only, as cell control. The plates were then incubated for 30 minutes at room temperature. 100 µL of the virus/sample mix or virus or medium alone was then added to the cells and spinoculated by centrifugation at 1250 rpm for 1 hour at room temperature. After incubation for 18 to 22 hours at 37°C, the measurement of infection/neutralization was performed as described for the COV2pp titration.

The percentage of neutralization was calculated with the formula: 100-((sample's R.L.U. – cell control

R.L.U.) / virus control R.L.U.) *100). The inhibitory concentration 50% (IC_{50}) and 90% (IC_{90}) were respectively defined as the reciprocal sample dilution or purified Ig fraction concentration achieving 50% and 90% neutralization.

Statistical analysis. The statistical significance was determined by a two-tailed Mann-Whitney test and correlations analyzed with a Spearman rank-order correlation test using GraphPad Prism 8.

Data availability.

The raw data that support the findings of this study are available from the corresponding author upon request.

References.

1. Zhu, N. *et al.* A Novel Coronavirus from Patients with Pneumonia in China, 2019. *N. Engl. J. Med.* **382**, 727–733 (2020).

2. WHO Coronavirus Disease (COVID-19) Dashboard. https://covid19.who.int.

3. Liu, S. T. H. *et al.* Convalescent plasma treatment of severe COVID-19: A matched control study. *medRxiv* 2020.05.20.20102236 (2020) doi:10.1101/2020.05.20.20102236.

4. Pei, S. *et al.* Convalescent Plasma to Treat COVID-19: Chinese Strategy and Experiences. *medRxiv* 2020.04.07.20056440 (2020) doi:10.1101/2020.04.07.20056440.

5. Martinez-Resendez, M. F. *et al.* Initial experience in Mexico with convalescent plasma in COVID-19 patients with severe respiratory failure, a retrospective case series. *medRxiv* 2020.07.14.20144469 (2020) doi:10.1101/2020.07.14.20144469.

6. Le, T. T. *et al.* The COVID-19 vaccine development landscape. *Nat. Rev. Drug Discov.* **19**, 305–306 (2020).

7. Amanat, F. & Krammer, F. SARS-CoV-2 Vaccines: Status Report. *Immunity* (2020)

doi:10.1016/j.immuni.2020.03.007.

8. Mulligan, M. J. *et al.* Phase 1/2 Study to Describe the Safety and Immunogenicity of a COVID-19 RNA Vaccine Candidate (BNT162b1) in Adults 18 to 55 Years of Age: Interim Report. *medRxiv* 2020.06.30.20142570 (2020) doi:10.1101/2020.06.30.20142570.

9. Yu, J. *et al.* DNA vaccine protection against SARS-CoV-2 in rhesus macaques. *Science* (2020) doi:10.1126/science.abc6284.

10. Yan, R. *et al.* Structural basis for the recognition of SARS-CoV-2 by full-length human ACE2. *Science* **367**, 1444–1448 (2020).

11. Hoffmann, M. *et al.* The novel coronavirus 2019 (2019-nCoV) uses the SARS-coronavirus receptor ACE2 and the cellular protease TMPRSS2 for entry into target cells. *bioRxiv* 2020.01.31.929042 (2020) doi:10.1101/2020.01.31.929042.

12. Wang, K. *et al.* SARS-CoV-2 invades host cells via a novel route: CD147-spike protein. *bioRxiv* 2020.03.14.988345 (2020) doi:10.1101/2020.03.14.988345.

13. Cantuti-Castelvetri, L. *et al.* Neuropilin-1 facilitates SARS-CoV-2 cell entry and provides a possible pathway into the central nervous system. *bioRxiv* 2020.06.07.137802 (2020) doi:10.1101/2020.06.07.137802.

14. Zhou, P. *et al.* A pneumonia outbreak associated with a new coronavirus of probable bat origin. *Nature* **579**, 270–273 (2020).

15. Lu, R. *et al.* Genomic characterisation and epidemiology of 2019 novel coronavirus: implications for virus origins and receptor binding. *Lancet Lond. Engl.* **395**, 565–574 (2020).

16. Hoffmann, M. *et al.* SARS-CoV-2 Cell Entry Depends on ACE2 and TMPRSS2 and Is Blocked by a Clinically Proven Protease Inhibitor. *Cell* **181**, 271-280.e8 (2020).

17. Walls, A. C. *et al.* Structure, Function, and Antigenicity of the SARS-CoV-2 Spike Glycoprotein. *Cell* **181**, 281-292.e6 (2020).

18. Vidarsson, G., Dekkers, G. & Rispens, T. IgG Subclasses and Allotypes: From Structure to Effector Functions. *Front. Immunol.* **5**, (2014).

19. Schroeder, H. W. & Cavacini, L. Structure and function of immunoglobulins. *J. Allergy Clin. Immunol.* **125**, S41-52 (2010).

20. Boes, M. Role of natural and immune IgM antibodies in immune responses. *Mol. Immunol.* **37**, 1141–1149 (2000).

21. Müller, R. *et al.* High-resolution structures of the IgM Fc domains reveal principles of its hexamer formation. *Proc. Natl. Acad. Sci.* **110**, 10183–10188 (2013).

22. Brekke, O. H. & Sandlie, I. Therapeutic antibodies for human diseases at the dawn of the twenty-first century. *Nat. Rev. Drug Discov.* **2**, 52–62 (2003).

23. Ma, H. *et al.* Serum IgA, IgM, and IgG responses in COVID-19. *Cell. Mol. Immunol.* **17**, 773–775 (2020).

24. Grifoni, A. *et al.* Targets of T Cell Responses to SARS-CoV-2 Coronavirus in Humans with COVID-19 Disease and Unexposed Individuals. *Cell* **181**, 1489-1501.e15 (2020).

25. Long, Q.-X. *et al.* Antibody responses to SARS-CoV-2 in patients with COVID-19. *Nat. Med.* **26**, 845–848 (2020).

26. Robbiani, D. F. *et al.* Convergent antibody responses to SARS-CoV-2 in convalescent individuals. *Nature* (2020) doi:10.1038/s41586-020-2456-9.

27. Zhao, J. *et al.* Antibody responses to SARS-CoV-2 in patients of novel coronavirus disease 2019. *Clin. Infect. Dis. Off. Publ. Infect. Dis. Soc. Am.* (2020) doi:10.1093/cid/ciaa344.

28. Okba, N. M. A. *et al.* Severe Acute Respiratory Syndrome Coronavirus 2-Specific Antibody Responses in Coronavirus Disease Patients. *Emerg. Infect. Dis.* **26**, 1478–1488 (2020).

29. Guo, L. *et al.* Profiling Early Humoral Response to Diagnose Novel Coronavirus Disease (COVID-19). *Clin. Infect. Dis. Off. Publ. Infect. Dis. Soc. Am.* (2020) doi:10.1093/cid/ciaa310.

30. Padoan, A. *et al.* IgA-Ab response to spike glycoprotein of SARS-CoV-2 in patients with COVID-19: A longitudinal study. *Clin. Chim. Acta* **507**, 164–166 (2020).

31. Ju, B. *et al.* Human neutralizing antibodies elicited by SARS-CoV-2 infection. *Nature* (2020) doi:10.1038/s41586-020-2380-z.

32. Wu, F. *et al.* Neutralizing antibody responses to SARS-CoV-2 in a COVID-19 recovered patient cohort and their implications. *medRxiv* 2020.03.30.20047365 (2020) doi:10.1101/2020.03.30.20047365.

33. Rogers, T. F. *et al.* Isolation of potent SARS-CoV-2 neutralizing antibodies and protection from disease in a small animal model. *Science* (2020) doi:10.1126/science.abc7520.

34. Zost, S. J. *et al.* Potently neutralizing and protective human antibodies against SARS-CoV-2. *Nature* 1–10 (2020) doi:10.1038/s41586-020-2548-6.

35. Ejemel, M. *et al.* IgA MAb blocks SARS-CoV-2 Spike-ACE2 interaction providing mucosal immunity. *BioRxiv Prepr. Serv. Biol.* (2020) doi:10.1101/2020.05.15.096719.

36. Renegar, K. B., Small, P. A., Boykins, L. G. & Wright, P. F. Role of IgA versus IgG in the control of influenza viral infection in the murine respiratory tract. *J. Immunol. Baltim. Md 1950* **173**, 1978–1986 (2004).

37. Suzuki, T. *et al.* Relationship of the quaternary structure of human secretory IgA to neutralization of influenza virus. *Proc. Natl. Acad. Sci. U. S. A.* **112**, 7809–7814 (2015).

38. Krammer, F. The human antibody response to influenza A virus infection and vaccination. *Nat. Rev. Immunol.* **19**, 383–397 (2019).

39. Reynolds, H. Y. Immunoglobulin G and its function in the human respiratory tract. *Mayo Clin. Proc.* **63**, 161–174 (1988).

40. Muramatsu, M. *et al.* Comparison of antiviral activity between IgA and IgG specific to influenza virus hemagglutinin: increased potential of IgA for heterosubtypic immunity. *PloS One* **9**, e85582 (2014).

41. Shen, C. *et al.* An IgM antibody targeting the receptor binding site of influenza B blocks viral infection with great breadth and potency. *Theranostics* **9**, 210–231 (2019).

42. Habibi, M. S. *et al.* Impaired Antibody-mediated Protection and Defective IgA B-Cell Memory in Experimental Infection of Adults with Respiratory Syncytial Virus. *Am. J. Respir. Crit. Care Med.* **191**, 1040–1049 (2015).

43. Du, L. *et al.* The spike protein of SARS-CoV--a target for vaccine and therapeutic development. *Nat. Rev. Microbiol.* **7**, 226–236 (2009).

44. Weiss, S. *et al.* A High Through-put Assay for Circulating Antibodies Directed against the S Protein of Severe Acute Respiratory Syndrome Corona virus 2. *medRxiv* 2020.04.14.20059501 (2020) doi:10.1101/2020.04.14.20059501.

45. Oguntuyo, K. Y. *et al.* Quantifying absolute neutralization titers against SARS-CoV-2 by a standardized virus neutralization assay allows for cross-cohort comparisons of COVID-19 sera. *medRxiv* 2020.08.13.20157222 (2020) doi:10.1101/2020.08.13.20157222.

46. Yang, J. *et al.* A vaccine targeting the RBD of the S protein of SARS-CoV-2 induces protective immunity. *Nature* (2020) doi:10.1038/s41586-020-2599-8.

47. Zhu, F.-C. *et al.* Immunogenicity and safety of a recombinant adenovirus type-5-vectored COVID-19 vaccine in healthy adults aged 18 years or older: a randomised, double-blind, placebo-controlled, phase 2 trial. *Lancet Lond. Engl.* (2020) doi:10.1016/S0140-6736(20)31605-6.

48. Jackson, L. A. *et al.* An mRNA Vaccine against SARS-CoV-2 — Preliminary Report. *N. Engl. J. Med.* **0**, null (2020).

49. Patel, A. *et al.* Intradermal-delivered DNA vaccine provides anamnestic protection in a rhesus macaque SARS-CoV-2 challenge model. *bioRxiv* 2020.07.28.225649 (2020) doi:10.1101/2020.07.28.225649.

50. Mercado, N. B. *et al.* Single-shot Ad26 vaccine protects against SARS-CoV-2 in rhesus

macaques. *Nature* (2020) doi:10.1038/s41586-020-2607-z.

51. Zeng, F. *et al.* A comparison study of SARS-CoV-2 IgG antibody between male and female COVID-19 patients: a possible reason underlying different outcome between gender. *medRxiv* 2020.03.26.20040709 (2020) doi:10.1101/2020.03.26.20040709.

52. Fink, A. L., Engle, K., Ursin, R. L., Tang, W.-Y. & Klein, S. L. Biological sex affects vaccine efficacy and protection against influenza in mice. *Proc. Natl. Acad. Sci. U. S. A.* **115**, 12477–12482 (2018).

53. Potluri, T. *et al.* Age-associated changes in the impact of sex steroids on influenza vaccine responses in males and females. *Npj Vaccines* **4**, 1–12 (2019).

54. Jin, J.-M. *et al.* Gender Differences in Patients With COVID-19: Focus on Severity and Mortality. *Front. Public Health* **8**, (2020).

55. Long, Q.-X. *et al.* Clinical and immunological assessment of asymptomatic SARS-CoV-2 infections. *Nat. Med.* 1–5 (2020) doi:10.1038/s41591-020-0965-6.

56. Horwitz *et al.* Non-neutralizing Antibodies Alter the Course of HIV-1 Infection In Vivo. *Cell* (2017) doi:10.1016/j.cell.2017.06.048.

57. Chung, A. W. *et al.* Polyfunctional Fc-effector profiles mediated by IgG subclass selection distinguish RV144 and VAX003 vaccines. *Sci. Transl. Med.* **6**, 228ra38 (2014).

58. Ilinykh, P. A. *et al.* Non-neutralizing Antibodies from a Marburg Infection Survivor Mediate Protection by Fc-Effector Functions and by Enhancing Efficacy of Other Antibodies. *Cell Host Microbe* **27**, 976-991.e11 (2020).

59. Gunn, B. M. *et al.* A Role for Fc Function in Therapeutic Monoclonal Antibody-Mediated Protection against Ebola Virus. *Cell Host Microbe* **24**, 221-233.e5 (2018).

60. Zohar, T. & Alter, G. Dissecting antibody-mediated protection against SARS-CoV-2. *Nat. Rev. Immunol.* **20**, 392–394 (2020).

61. Pinto, D. *et al.* Cross-neutralization of SARS-CoV-2 by a human monoclonal SARS-CoV antibody. *Nature* **583**, 290–295 (2020).

62. Atyeo, C. *et al.* Distinct Early Serological Signatures Track with SARS-CoV-2 Survival. *Immunity* (2020) doi:10.1016/j.immuni.2020.07.020.

63. Meyer-Bahlburg, A. B-1 cells as a source of IgA. *Ann. N. Y. Acad. Sci.* **1362**, 122–131 (2015).

64. Rodriguez-Zhurbenko, N., Quach, T. D., Hopkins, T. J., Rothstein, T. L. & Hernandez, A. M. Human B-1 Cells and B-1 Cell Antibodies Change With Advancing Age. *Front. Immunol.* **10**, (2019).

65. Amanat, F. *et al.* A serological assay to detect SARS-CoV-2 seroconversion in humans. *Nat. Med.* 1–4 (2020) doi:10.1038/s41591-020-0913-5.

66. Stadlbauer, D. *et al.* SARS-CoV-2 Seroconversion in Humans: A Detailed Protocol for a Serological Assay, Antigen Production, and Test Setup. *Curr. Protoc. Microbiol.* **57**, e100 (2020).

Funding

This study was supported by the Microbiology Laboratory Clinical Services at the Mount Sinai Health System and the Mount Sinai Health System Translational Science Hub, National Institutes of Health [grant U54TR001433]; the Personalized Virology Initiative supported by institutional funds and philanthropic donations (to V.S.); the Department of Medicine of the Icahn School of Medicine at Mount Sinai Department of Medicine (to S.Z-P., C.E.H.); the Department of Microbiology and the Ward-Coleman estate for endowing the Ward-Coleman Chairs at the Icahn School of Medicine at Mount Sinai (to B.L.), the National Institute of Allergy and Infectious Diseases Centers of Excellence for Influenza Research and Surveillance [contract HHSN272201400008C] (to F.K., V.S.); the Department of Veterans Affairs [Merit Review Grant I01BX003860] (to C.E.H.) and [Research Career Scientist Award 1IK6BX004607] (to C.E.H.); the National Institute of Allergy and Infectious Diseases [grant AI139290] to C.E.H., [grant AI136916] (to V.S.), [grants R01 AI123449, R21 AI1498033] to B.L. K.Y.O. and C.S. were supported by Viral-Host Pathogenesis Training Grant T32 AI07647; K.Y.O. was additionally supported by F31 AI154739. S.I. and C-T. H. were supported by postdoctoral fellowships from CHOT-SG (Fukuoka University, Japan) and the Ministry of Science and Technology (MOST, Taiwan), respectively.

Acknowledgments

We thank all the donors for their contribution to research and Dr. Arthur Nadas (NYU School of Medicine) for statistical consultation.

Competing interests

The authors declare no competing interests.

Author contributions

J.K., S.W., G.E-A., S.Z-P., and C.E.H. wrote and edited the manuscript. S.W., J.K., C.E.H., and S.Z-P. designed the experiments. J.K., S.W., V.I., X.L. performed the experiments and collected the data. J.K., S.Z-P. and C.E.H. analyzed the data. K.Y.O., C.S., S.I., C-T.H., F.A., B.L., and F.K. provided protocols, antigens, cells and pseudovirus stocks. G.E-A., I.B., S.A., J.C.B., E.M.K., J.S., S.L., D.J., M.B-G., and V.S. provided samples. All authors read and approved the final manuscript.

Figure legends

Fig. 1. Titration of SARS-CoV-2 spike and RBD total Ig in plasma or serum samples from COVID-19 convalescent individuals. Titration of (a) spike-specific or (b) RBD-specific total Ig from 29 COVID-19-convalescent individuals, two COVID-19 patients with longitudinal samples, and 13 COVID-19-negative individuals. Specimens were diluted at 2-fold dilutions from 1:50 to 1:6,400.

Fig. 2. Levels of Ig isotypes against the SARS-CoV-2 spike and RBD vary in plasma or serum samples from COVID-19 convalescent individuals. Detection of total Ig, IgM, IgG1, IgG2, IgG3, IgG4, IgA1 and IgA2 against (a) spike and (b) RBD in specimens from 29 COVID-19-convalescent individuals and 13 COVID-19-negative individuals. The samples were tested at a dilution of 1:200 and data are shown as mean MFI + standard deviation (SD) of duplicate measurements from at least two independent experiments. The horizontal red dotted line represents the cut-off value determined as the mean of all negative samples + 3 SD for each of the isotypes. (c) Percentages of responders above the cut-off for each spike- or RBD-specific Ig isotype.

Fig. 3. Correlation of total Ig with IgG1, the dominant isotype response induced in COVID-19 convalescent individuals. Spearman correlations of (a) spike-specific or (b) RBD-specific total Ig levels versus IgM, IgG1 or IgA1 levels or (c) spike-specific and RBD-specific IgG1, IgA1, and IgM levels with one another from the 29 COVID-19-convalescent individuals from Fig. 1.

Fig. 4. Induction of IgA1 and IgG1 along with IgM early after disease onset. Kinetics of induction of (a) spike-specific or (b) RBD-specific total Ig, IgM, IgG1, IgG2, IgG3, IgG4, IgA1, and IgA2 from two COVID-19 patients. Longitudinal samples from each patient were tested at a dilution of 1:200 in parallel with all negative samples and data are shown as mean MFI + SD of duplicate measurements from at least two experiments. The dotted red line represents the cut-off value calculated as the mean of all negative samples + 3 SD from Fig. 1.

Fig. 5. Neutralization activities detected in all COVID-19 convalescent individuals. Neutralization

of COV2pp by samples from (a) 28 COVID-19-convalescent individuals and (b) 11 COVID-19-negative individuals, compared to (c) a recombinant soluble RBD (sRBD) control. Each plasma or sera specimen was tested at 4-fold dilutions from 1:10 to 1:40,960, and sRBD was tested at 4-fold dilutions from 100 to 0.02 µg/mL. The data are shown as mean percentage of neutralization + SD of triplicate. The extrapolated titration curves were generated using a nonlinear regression model in GraphPad Prism (Inhibitor versus response – variable slope (four parameters), least squares regression). The dotted horizontal lines highlight 50% neutralization.

Fig. 6. Summary of relative Ig isotype levels and neutralization titers. Table showing gender (F: female, M: male), relative levels of spike-specific and RBD-specific isotype levels (+: bottom quartile, ++: second quartile, +++: third quartile, ++++: top quartile, -: non-responder) and neutralization reciprocal IC_{50} and IC_{90} titers of 29 COVID-19-convalescent individuals (nd: not done).

Fig. 7. SARS-CoV-2 neutralization titers correlate with IgM and IgA1. (a) Spearman correlations of neutralization reciprocal IC_{90} titers versus spike-specific or RBD-specific total Ig, IgM, IgG1 and IgA1 Ab levels. The dotted vertical line represents the cut-off (mean of negative samples + 3 SD) for each isotype from Fig. 1. (b) Spearman correlations of neutralization reciprocal IC_{90} titers versus spike-specific or RBD-specific total IgG2-4 and IgA2 Ab levels.

Fig. 8. Purified IgM, IgG, and IgA fractions display neutralizing activities against SARS-CoV-2. (a) Neutralization of COV2pp by five COVID-19-infected individual plasma (RP#1-5) compared to a COVID-19-negative individual (RN#1). Plasma were tested at 4-fold dilutions from 1:10 to 1:40,960 or 1:20 to 1:81,920. Data are shown as the mean percentage of neutralization. The dotted horizontal lines highlight 50% neutralization. (b) Neutralization reciprocal IC_{50} and IC_{90} titers of RP#1-5 plasma. (c) Neutralization of COV2pp by purified IgM, IgG, and IgA fractions from 5 COVID-19-infected individual plasma (RP#1-5) compared to a control Ig fraction. The fractions were tested at 4-fold dilutions from 500 to 0.02 µg/mL. Data are shown as the mean percentage of neutralization. The dotted

horizontal lines highlight 50% neutralization. (d) IC_{50} of purified IgM, IgG, and IgA fractions from RP#1-5 plasma. The statistical significance was determined by a two-tailed Mann-Whitney test (*: $p < 0.05$, **: $p < 0.01$).

Supplementary Fig. 1. Spearman correlations of the area under the curves (AUCs) of (a) spike- or (b) RBD-specific total Ig versus total Ig MFI values at a 1:200 dilution.

Supplementary Fig. 2. Spearman correlations between (a) spike-specific or (b) RBD-specific total Ig MFI values from two independent experiments to show the degree of assay reproducibility.

Supplementary Fig. 3. Isotyping validation was performed by coating Luminex beads with IgG1, IgG2, IgG3, IgG4, IgA1, IgA2, and IgM myeloma proteins and detecting each specifically with eight different secondary Abs against (a) total Ig, (b) IgM, (c) IgG1, (d) IgG2, (e) IgG3, (f) IgG4, (g) IgA1 and (h) IgA2. The data are shown as mean MFI + SD of duplicate.

Supplementary Fig. 4. Spearman correlations between spike-specific versus RBD-specific total Ig, IgM, IgG1, IgG2, IgG3, IgG4, IgA1, or IgA2 MFI values.

Supplementary Fig. 5. Violin plots of (a) spike-specific or (b) RBD-specific total Ig, IgM, IgG1, and IgA1 levels from nine COVID-19 convalescent female (F) and 15 male (M) subjects. The statistical significance was determined by a two-tailed Mann-Whitney test (ns: non-significant: $p > 0.05$).

Supplementary Fig. 6. Enrichment of spike-specific IgM (a), IgG (b), and IgA in purified fractions from RP#1-5 and RN#1. Each fraction was measured for the presence of IgM, IgG1, IgG2, IgG3, IgG4, IgA1, and IgA2 Abs using the isotyping method validated in Supplementary Fig. 3.

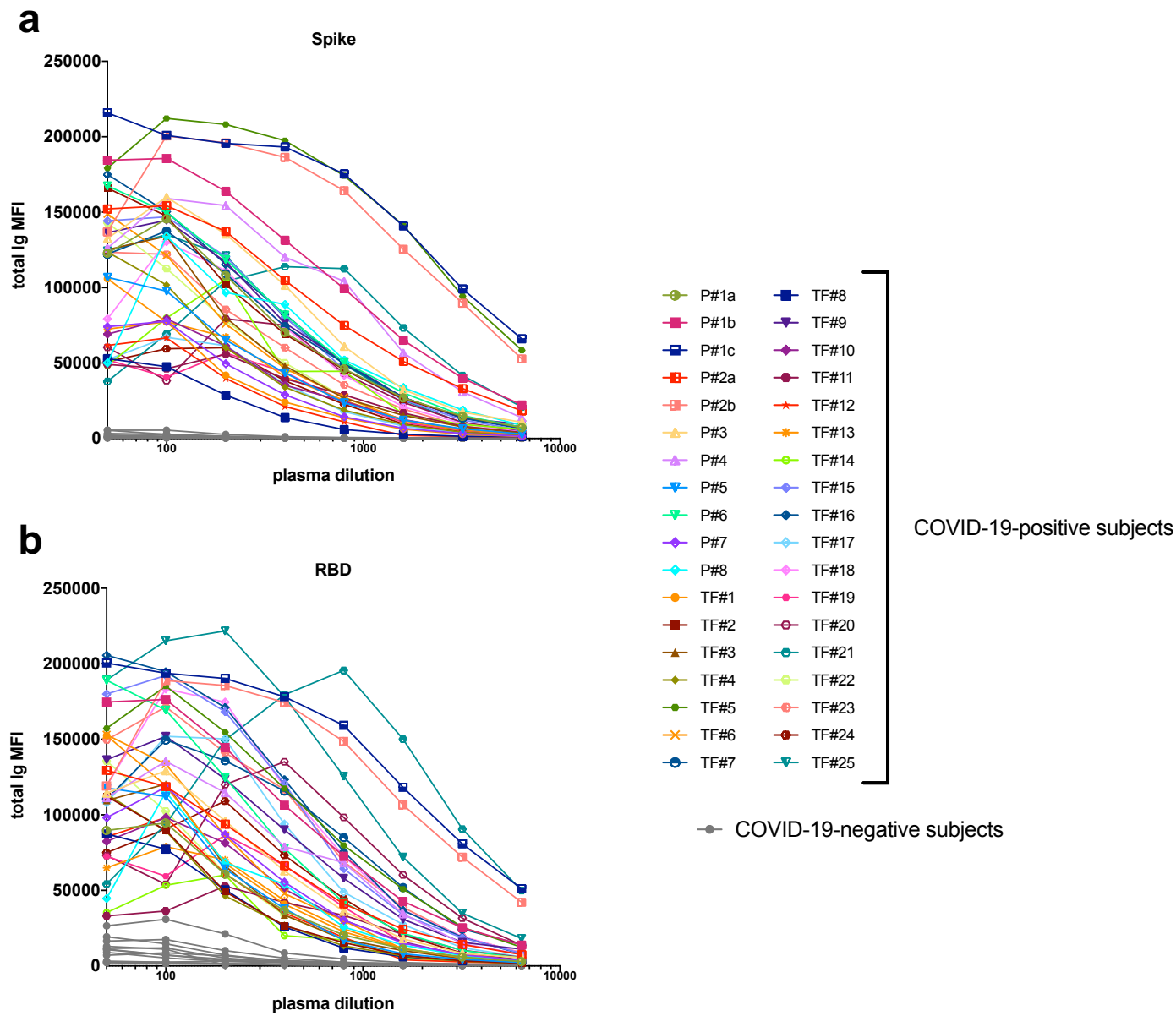
a
Spike
total Ig MFI
250000
200000
150000
100000
50000
0
100
1000
10000
plasma dilution
b
RBD
total Ig MFI
250000
200000
150000
100000
50000
0
100
1000
10000
plasma dilution
P#1a
P#1b
P#1c
P#2a
P#2b
P#3
P#4
P#5
P#6
P#7
P#8
TF#1
TF#2
TF#3
TF#4
TF#5
TF#6
TF#7
TF#8
TF#9
TF#10
TF#11
TF#12
TF#13
TF#14
TF#15
TF#16
TF#17
TF#18
TF#19
TF#20
TF#21
TF#22
TF#23
TF#24
TF#25
COVID-19-positive subjects
COVID-19-negative subjects

Fig. 1. Titration of SARS-CoV-2 spike and RBD total Ig in plasma or serum samples from COVID-19 convalescent individuals. Titration of (a) spike-specific or (b) RBD-specific total Ig from 29 COVID-19-convalescent individuals, two COVID-19 patients with longitudinal samples, and 13 COVID-19-negative individuals. Specimens were diluted at 2-fold dilutions from 1:50 to 1:6,400.

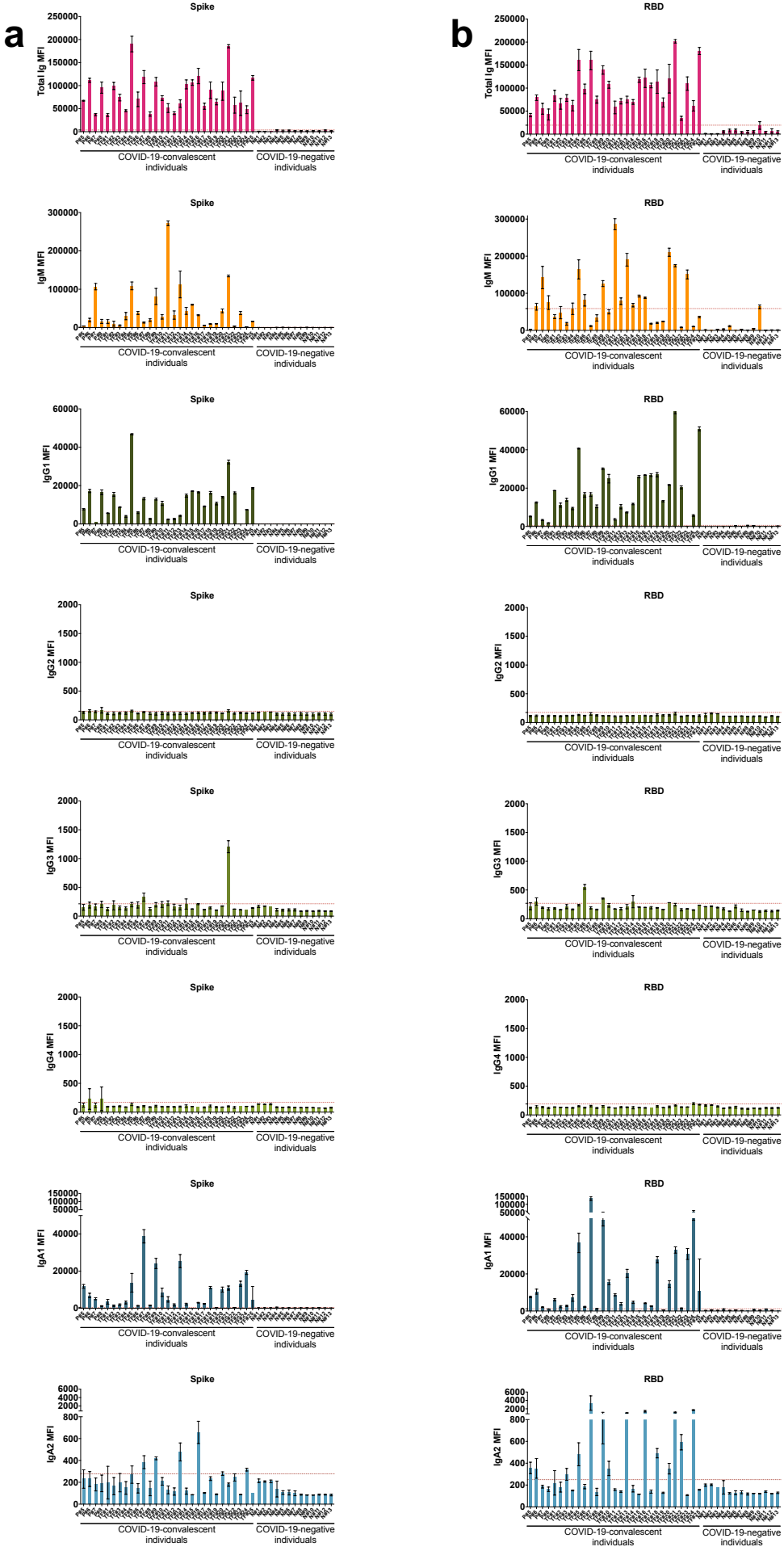

c

	Spike	RBD
Total Ig	100%	100%
IgM	100%	55%
IgG1	97%	97%
IgG2	14%	0%
IgG3	10%	17%
IgG4	7%	3%
IgA1	90%	86%
IgA2	21%	48%

Fig. 2. Levels of Ig isotypes against the SARS-CoV-2 spike and RBD vary in plasma or serum samples from COVID-19 convalescent individuals. Detection of total Ig, IgM, IgG1, IgG2, IgG3, IgG4, IgA1 and IgA2 against (a) spike and (b) RBD in specimens from 29 COVID-19-convalescent individuals and 13 COVID-19-negative individuals. The samples were tested at a dilution of 1:200 and data are shown as mean MFI + standard deviation (SD) of duplicate measurements from at least two independent experiments. The horizontal red dotted line represents the cut-off value determined as the mean of all negative samples + 3 SD for each of the isotypes. (c) Percentages of responders above the cut-off for each spike- or RBD-specific Ig isotype.

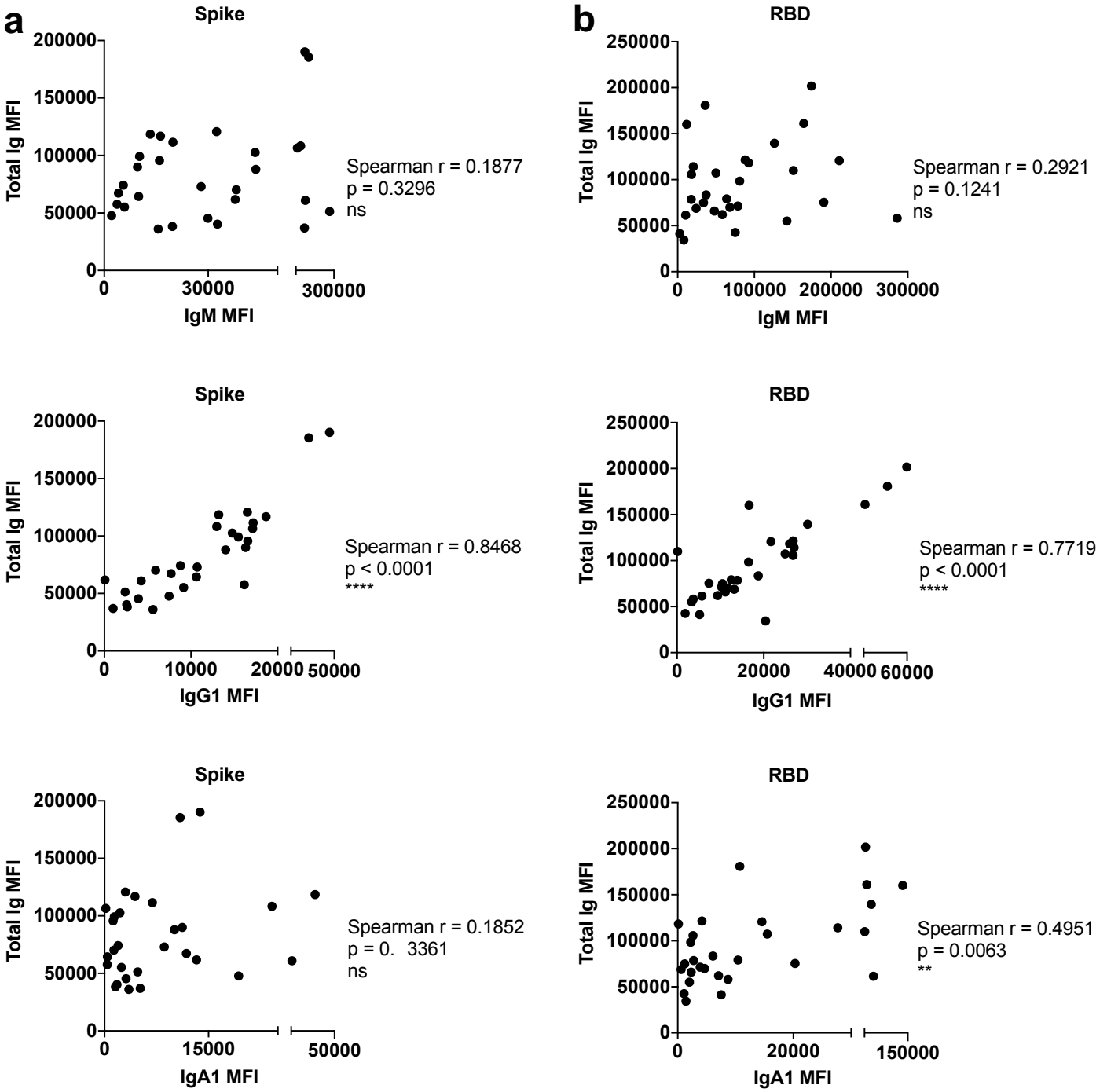

c

	Spike			RBD		
	Spearman r	p		Spearman r	p	
IgG1 vs IgM	-0.04236	0.8273	ns	-0.0133	0.9535	ns
IgG1 vs IgA1	-0.06207	0.7491	ns	0.2236	0.2435	ns
IgA1 vs IgM	0.2143	0.2643	ns	0.1562	0.4186	ns

Fig. 3. Correlation of total Ig with IgG1, the dominant isotype response induced in COVID-19 convalescent individuals. Spearman correlations of (a) spike-specific or (b) RBD-specific total Ig levels versus IgM, IgG1 or IgA1 levels or (c) spike-specific and RBD-specific IgG1, IgA1, and IgM levels with one another from the 29 COVID-19-convalescent individuals from Fig. 1.

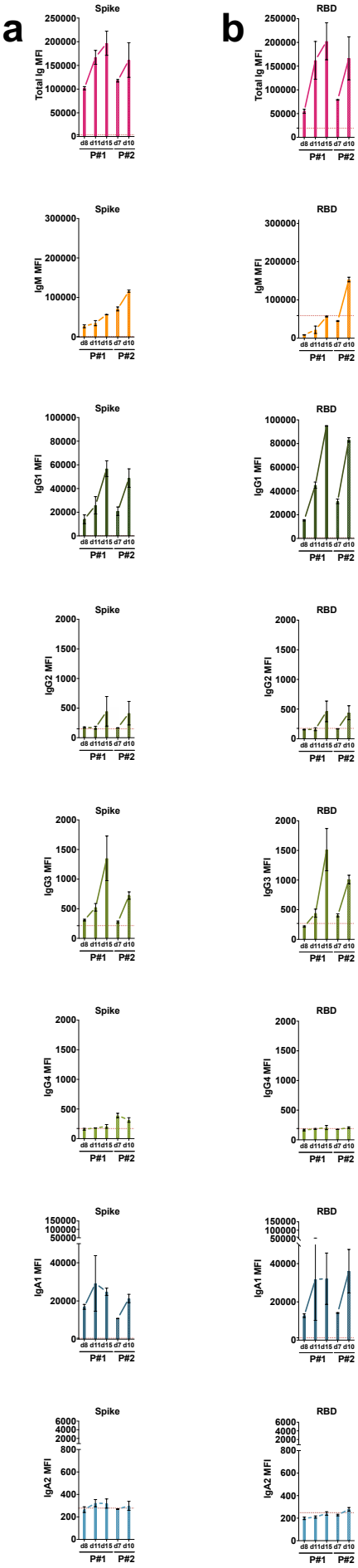
a
b
Spike
RBD
Total Ig MFI
IgM MFI
IgG1 MFI
IgG2 MFI
IgG3 MFI
IgG4 MFI
IgA1 MFI
IgA2 MFI
d8 d11 d15 d7 d10
P#1
P#2

Fig. 4. Induction of IgA1 and IgG1 along with IgM early after disease onset. Kinetics of induction of (a) spike-specific or (b) RBD-specific total Ig, IgM, IgG1, IgG2, IgG3, IgG4, IgA1, and IgA2 from two COVID-19 patients. Longitudinal samples from each patient were tested at a dilution of 1:200 in parallel with all negative samples and data are shown as mean MFI + SD of duplicate measurements from at least two experiments. The dotted red line represents the cut-off value calculated as the mean of all negative samples + 3 SD from Fig. 1.

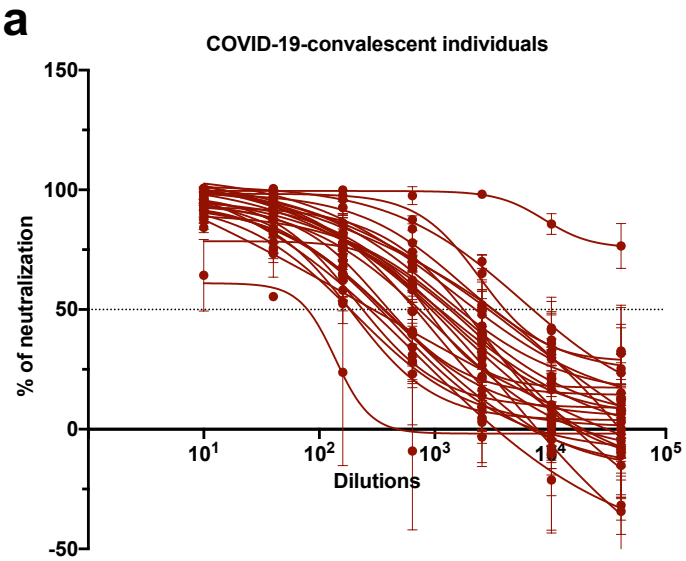
a
COVID-19-convalescent individuals
% of neutralization
150
100
50
0
-50
10^1
10^2
10^3
10^4
10^5
Dilutions

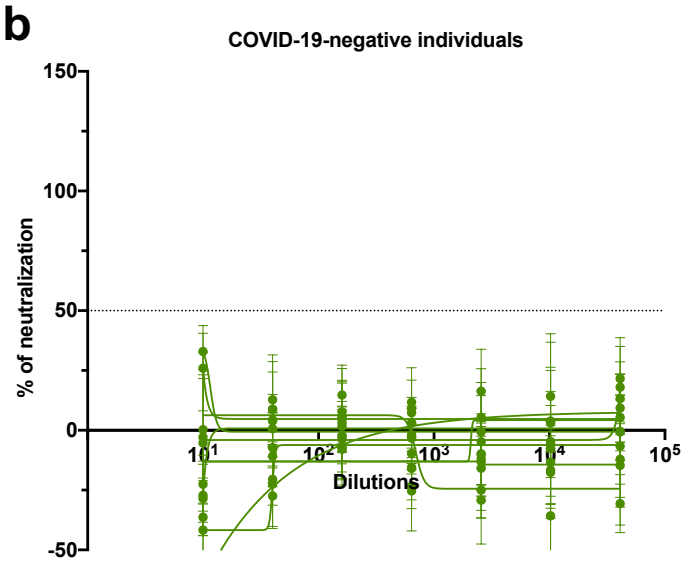
b
COVID-19-negative individuals
% of neutralization
150
100
50
0
-50
10^1
10^2
10^3
10^4
10^5
Dilutions

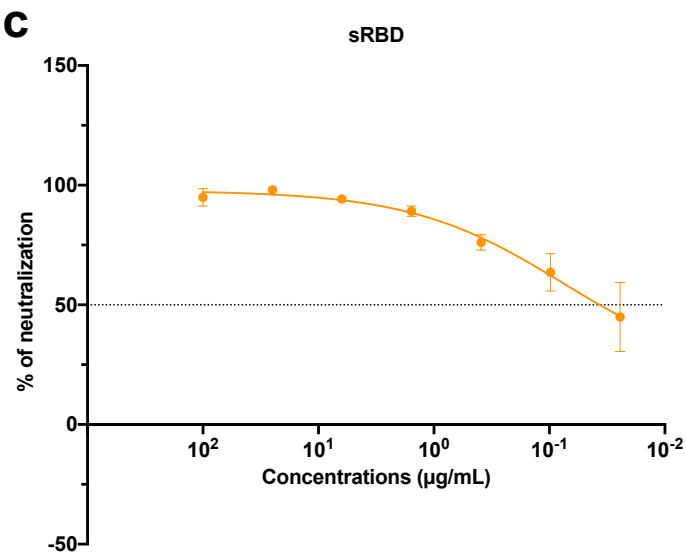
c
sRBD
% of neutralization
150
100
50
0
-50
10^2
10^1
10^0
10^{-1}
10^{-2}
Concentrations (µg/mL)

Fig. 5. Neutralization activities detected in all COVID-19 convalescent individuals. Neutralization of COV2pp by samples from (a) 28 COVID-19-convalescent individuals and (b) 11 COVID-19-negative individuals, compared to (c) a recombinant soluble RBD (sRBD) control. Each plasma or sera specimen was tested at 4-fold dilutions from 1:10 to 1:40,960, and sRBD was tested at 4-fold dilutions from 100 to 0.02 μg/mL. The data are shown as mean percentage of neutralization + SD of triplicate. The extrapolated titration curves were generated using a nonlinear regression model in GraphPad Prism (Inhibitor versus response – variable slope (four parameters), least squares regression). The dotted horizontal lines highlight 50% neutralization.

	Gender	Spike								RBD								Neutralization	
		Total Ig	IgM	IgG1	IgG2	IgG3	IgG4	IgA1	IgA2	Total Ig	IgM	IgG1	IgG2	IgG3	IgG4	IgA1	IgA2	IC50	IC90
P#5	unknown	++	+	+	-	-	-	++	-	+	-	+	-	-	-	+	+	36.6	2.3
P#6	unknown	+++	+	++	+	-	+	+	-	++	+	+	-	+	-	+	+	561.0	25.6
P#7	unknown	+	++	+	-	-	-	+	-	++	++	+	-	-	-	+	-	nd	nd
P#8	unknown	++	+	++	+	-	+	+	-	+	++	+	-	-	-	-	-	376.2	10.2
TF#1	F	+	+	+	-	-	-	+	-	++	-	++	-	-	-	+	-	418.8	21.5
TF#2	M	++	+	++	-	-	-	+	-	++	-	+	-	-	-	+	-	177.5	11.8
TF#3	M	++	+	+	-	-	-	+	-	++	-	+	-	-	-	+	+	164.7	19.8
TF#4	F	+	+	+	-	-	-	+	-	++	+	+	-	-	-	+	-	998.6	39.9
TF#5	M	++++	++	++++	+	-	-	++	-	++++	+++	+++	-	-	-	++	+	2344.7	515.9
TF#6	F	++	+	+	-	-	-	+	-	++	++	++	-	+	-	+	-	976.6	51.9
TF#7	F	+++	+	++	-	+	-	++++	+	++++	-	++	-	-	-	++++	+	5788.5	90.7
TF#8	M	+	+	+	-	-	-	+	-	++	-	+	-	-	-	+	-	2840.0	142.1
TF#9	F	+++	++	++	-	-	-	+++	+	+++	++	++	-	+	-	++	+	4044.1	116.5
TF#10	M	++	+	+	-	-	-	+	-	+++	-	++	-	-	-	+	+	1060.0	72.7
TF#11	M	++	++++	+	-	+	-	+	-	++	++++	+	-	-	-	+	-	> 40960	7200.0
TF#12	F	+	+	+	-	-	-	+	-	++	++	+	-	-	-	+	-	285.5	30.0
TF#13	M	++	++	+	-	-	-	+++	+	++	+++	+	-	-	-	+	+	1697.6	144.9
TF#14	M	+++	+	++	-	-	-	+	-	++	+	+	-	+	-	+	-	17078.5	201.4
TF#15	M	+++	+	++	-	-	-	-	-	+++	++	++	-	-	-	-	-	2006.2	29.6
TF#16	M	+++	+	++	-	-	-	+	+	+++	++	++	-	-	-	+	+	1330.7	106.2
TF#17	M	++	+	+	-	-	-	+	-	+++	-	++	-	-	-	+	-	198.0	27.2
TF#18	F	++	+	++	-	-	-	++	-	+++	-	++	-	-	-	+	+	1122.1	56.9
TF#19	M	++	+	+	-	-	-	-	-	++	-	+	-	-	-	-	-	326.2	17.7
TF#20	F	++	+	++	-	-	-	++	+	+++	+++	++	-	+	-	+	+	1535.3	72.4
TF#21	M	++++	++	+++	+	+	-	++	-	++++	+++	++++	-	-	-	+	+	5375.7	389.7
TF#22	M	++	+	++	-	-	-	-	-	+	-	++	-	-	-	+	+	623.2	4.8
TF#23	unknown	++	+	-	-	-	-	++	-	+++	+++	-	-	-	-	+	-	3881.9	107.8
TF#24	M	+	+	+	-	-	-	++	+	++	-	+	-	-	+	++	+	813.6	24.4
TF#25	F	+++	+	++	-	-	-	+	-	++++	-	++++	-	-	-	+	-	958.6	78.7

Fig. 6. Summary of relative Ig isotype levels and neutralization titers. Table showing gender (F: female, M: male), relative levels of spike-specific and RBD-specific isotype levels (+: bottom quartile, ++: second quartile, +++: third quartile, ++++: top quartile, -: non-responder) and neutralization reciprocal IC_{50} and IC_{90} titers of 29 COVID-19-convalescent individuals (nd: not done).

a

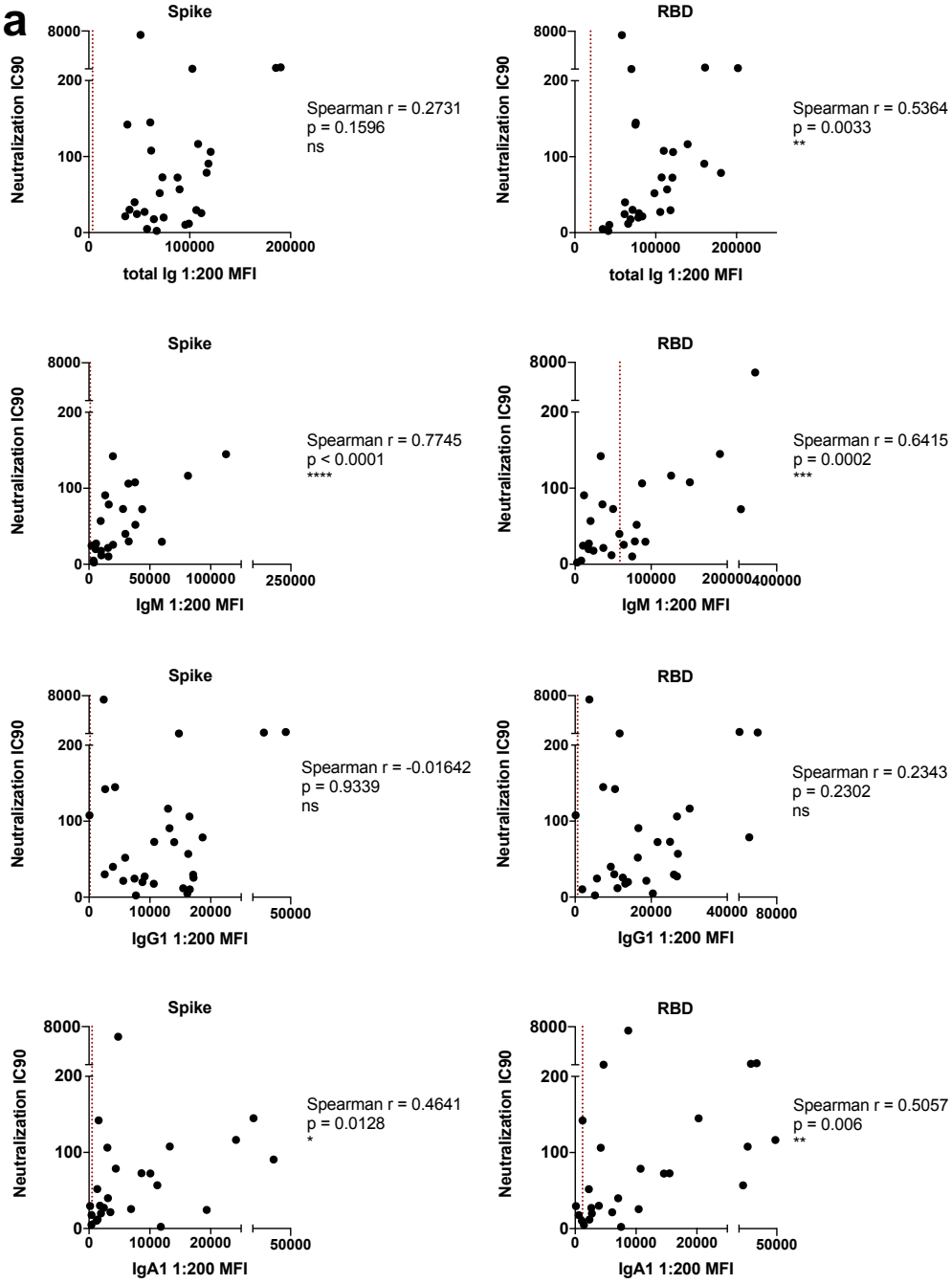

b

	Correlation IC_{90} versus spike MFI			Correlation IC_{90} versus RBD MFI		
	Spearman r	p		Spearman r	p	
IgG2	-0.1708	0.3849	ns	0.4423	0.0184	*
IgG3	0.4696	0.0117	*	0.3749	0.0493	*
IgG4	0.08211	0.6779	ns	0.1412	0.4735	ns
IgA2	0.06294	0.7503	ns	0.1193	0.5453	ns

Fig. 7. SARS-CoV-2 neutralization titers correlate with IgM and IgA1. (a) Spearman correlations of neutralization recriprocal IC_{90} titers versus spike-specific or RBD-specific total Ig, IgM, IgG1 and IgA1 Ab levels. The dotted vertical line represents the cut-off (mean of negative samples + 3 SD) for each isotype from Fig. 1. (b) Spearman correlations of neutralization reciprocal IC_{90} titers versus spike-specific or RBD-specific total IgG2-4 and IgA2 Ab levels.

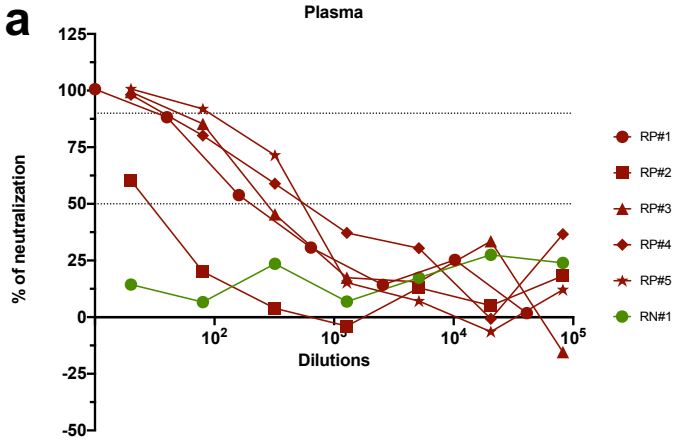

b

	Neutralization	
	IC50	IC90
RP#1	240	35
RP#2	35	< 20
RP#3	290	60
RP#4	690	45
RP#5	690	100

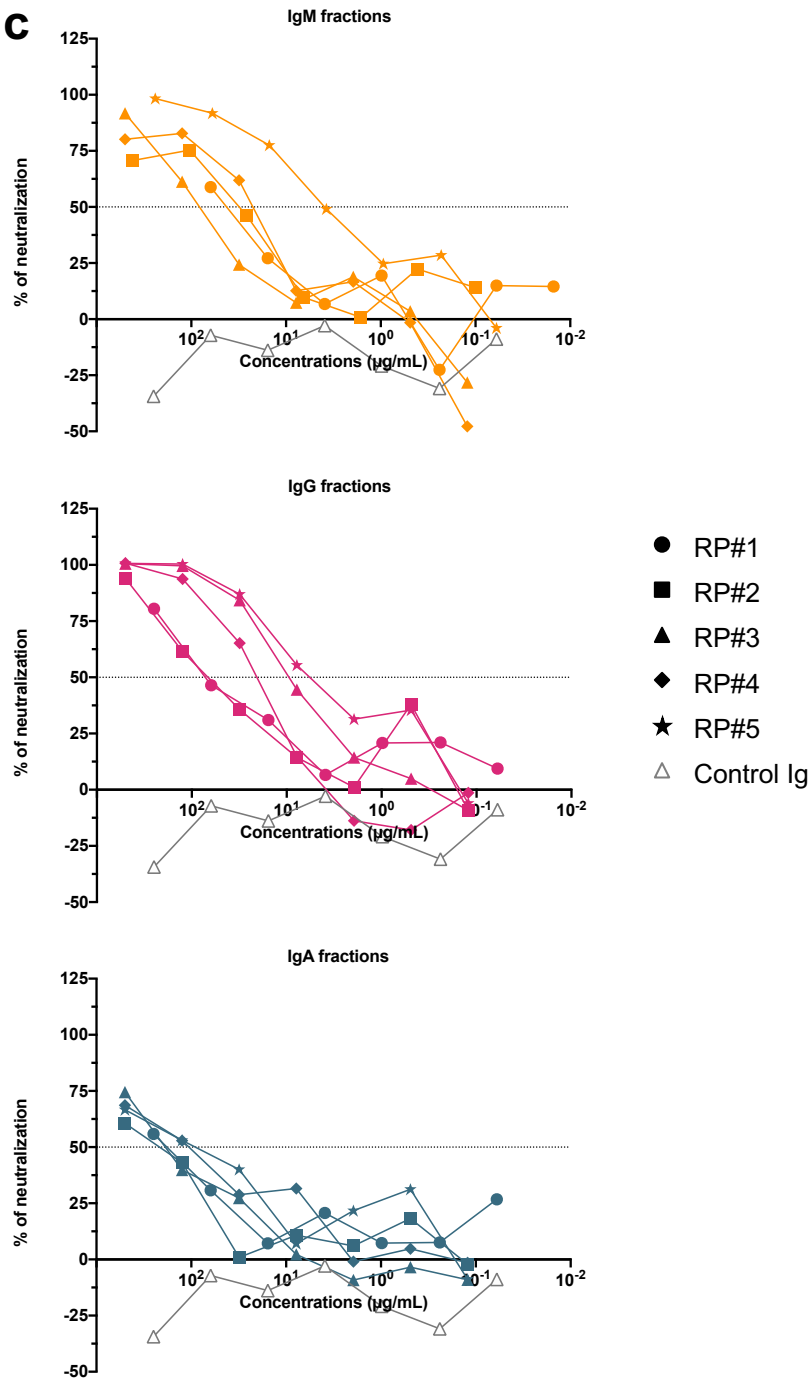

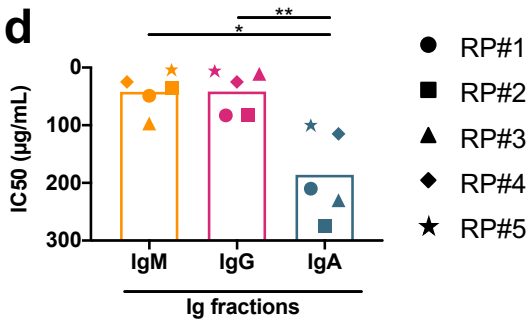

Fig. 8. Purified IgM, IgG, and IgA fractions display neutralizing activities against SARS-CoV-2. (a) Neutralization of COV2pp by five COVID-19-infected individual plasma (RP#1-5) compared to a COVID-19-negative individual (RN#1). Plasma were tested at 4-fold dilutions from 1:10 to 1:40,960 or 1:20 to 1:81,920. Data are shown as the mean percentage of neutralization. The dotted horizontal lines highlight 50% neutralization. (b) Neutralization reciprocal IC_{50} and IC_{90} titers of RP#1-5 plasma. (c) Neutralization of COV2pp by purified IgM, IgG, and IgA fractions from 5 COVID-19-infected individual plasma (RP#1-5) compared to a control Ig fraction. The fractions were tested at 4-fold dilutions from 500 to 0.02 μg/mL. Data are shown as the mean percentage of neutralization. The dotted horizontal lines highlight 50% neutralization. (d) IC_{50} of purified IgM, IgG, and IgA fractions from RP#1-5 plasma. The statistical significance was determined by a two-tailed Mann-Whitney test (*: $p < 0.05$, **: $p < 0.01$).